

This discussion paper is/has been under review for the journal Atmospheric Chemistry and Physics (ACP). Please refer to the corresponding final paper in ACP if available.

**IASI measurements
of tropospheric
ozone over Chinese
megacities**

G. Dufour et al.

IASI measurements of tropospheric ozone over Chinese megacities: Beijing, Shanghai, and Hong Kong

G. Dufour¹, M. Eremenko¹, J. Orphal^{1,2}, and J.-M. Flaud¹

¹Laboratoire Inter-universitaire des Systèmes Atmosphériques (LISA), UMR7583, Universités Paris-Est et Paris 7, CNRS, Créteil, France

²Institut für Meteorologie und Klimaforschung, Forschungszentrum Karlsruhe, Germany

Received: 7 August 2009 – Accepted: 19 October 2009 – Published: 2 November 2009

Correspondence to: G. Dufour (dufour@lisa.univ-paris12.fr)

Published by Copernicus Publications on behalf of the European Geosciences Union.

Title Page

Abstract

Introduction

Conclusions

References

Tables

Figures

⏪

⏩

◀

▶

Back

Close

Full Screen / Esc

Printer-friendly Version

Interactive Discussion

Abstract

IASI observations of tropospheric ozone over Beijing, Shanghai and Hong Kong during one year have been analysed, demonstrating the capability of space-borne infrared nadir measurements to probe both seasonal and daily variations of lower tropospheric ozone around megacities on the regional scale. The monthly variations of lower tropospheric ozone retrieved from IASI show the influence of the Asian summer monsoon that brings clean air masses from the Pacific during summer. They exhibit indeed a sharp ozone maximum in late spring and early summer (May–June) followed by a summer minimum. The time periods and the intensities of the maxima and of the decreases are latitude-dependent: they are more pronounced in Hong Kong and Shanghai than in Beijing. Moreover, IASI provides the opportunity to follow the spatial variations of ozone over the surroundings of each megacity as well as its daily variability. We show indeed that the large lower tropospheric ozone amounts observed with IASI are consistent with the highest population density distribution in each region, thus suggesting the anthropogenic origin of the large ozone amounts observed. Finally an analysis of the mean daily ozone profiles over each region for selected periods with high ozone events shows that the high ozone amounts observed during winter are likely related to descents of ozone-rich air from the stratosphere whereas in spring and summer the tropospheric ozone is likely enhanced by photochemical production in polluted areas and/or in fire plumes.

1 Introduction

Ozone (O_3) is a key trace gas in the troposphere that plays a significant role in atmospheric chemistry, air quality and atmospheric radiative forcing. It is not only an important greenhouse gas (Fishman et al., 1979), but also a secondary pollutant produced by the photochemical oxidation of hydrocarbons and carbon monoxide in presence of nitrogen oxide radicals ($NO+NO_2$). Ozone controls the oxidizing capacity of

IASI measurements of tropospheric ozone over Chinese megacities

G. Dufour et al.

Title Page

Abstract

Introduction

Conclusions

References

Tables

Figures

⏪

⏩

◀

▶

Back

Close

Full Screen / Esc

Printer-friendly Version

Interactive Discussion

the atmosphere being the primary precursor of the hydroxyl radical (OH) which is the main oxidant in the troposphere. Surface ozone at high concentrations is a pernicious pollutant that causes damages to human health and vegetation (Seinfeld and Pandis, 1997).

Background tropospheric ozone concentrations have been increasing for over a century especially in the Northern Hemisphere (Vingarzan, 2004). This increase is partly related to the growth of the emissions of ozone precursors (NO_x). Although trends in tropospheric ozone vary both in sign and in magnitude depending on the considered regions, background ozone levels in northern midlatitudes have continued to rise over the last decades (Vingarzan, 2004; Oltmans et al., 2006). In Europe, North America and Japan, tropospheric ozone levels increased in the 1970s and in the 1980s, but the increase has slowed down since the 1990s, and ozone levels even started to decrease in some regions, partly due to emission regulations applied in these countries (Oltmans et al., 2006). On the contrary, due to the rapid development of East Asia and in particular China, emissions of ozone precursors, that were still at low concentrations in the 1970s, have rapidly increased in the past decade (Richter et al., 2005) and are now larger than the North American and European emissions (Akimoto, 2003). Therefore, the tropospheric ozone amounts produced over China are then increasing, thus having a significant regional influence on the temporal and spatial variabilities of air quality in East Asia, but also up to the hemispheric scale due to the long-range transport across the Pacific (e.g. Jacob et al., 1999). Hence, monitoring of tropospheric ozone in this region of the world is important to better quantify its sources and its impact on air quality, in order to better evaluate its trend and the impact of long-range transport.

In the last years, the number of ozone measurements and studies focusing on China has significantly increased either through routine measurements (Chan et al., 1998; Xu et al., 1997; Ding et al., 2008; Lam et al., 2001; Lin et al., 2008, 2009; Wang et al., 2009) or through dedicated measurement campaigns (Liu et al., 1999) and through model studies (Liu et al., 2002; Li et al., 2007; He et al., 2008). The seasonal variations of surface ozone and the influence of the origin of the air masses and of the role

IASI measurements of tropospheric ozone over Chinese megacities

G. Dufour et al.

Title Page

Abstract

Introduction

Conclusions

References

Tables

Figures

⏪

⏩

◀

▶

Back

Close

Full Screen / Esc

Printer-friendly Version

Interactive Discussion

of the monsoon especially during summer have been studied for different regions of China (Xu et al., 1997; Liu et al., 2002; Ding et al., 2008; Lin et al., 2009). Also relatively long time-series of ozone measurements were reported for example for Hong Kong (e.g. Wang et al., 2009) and Beijing (e.g. Ding et al., 2008). However, these different studies are mainly based on surface or aircraft measurements with limited spatial coverage, leading to a persistent question about the representativeness of the sites at the regional scale.

The spatial coverage of the new generation of nadir-looking instruments onboard polar-orbiting satellites (e.g. IASI, GOME2, TES, OMI) makes them very promising tools to monitor tropospheric ozone over large regions, helping then to assess these problems related to air quality and transport. However retrieving tropospheric ozone from satellite observations is a challenging task because only a small part of the total atmospheric ozone is contained in the troposphere. The first satellite measurements of tropospheric ozone were obtained using ultraviolet-visible sounders (e.g. Fishmann et al., 2003; Liu et al., 2005) but this type of measurements has some limitations in the mid- and high latitudes. On the other hand, the recent development of infrared nadir sounders allows accurate measurements of tropospheric ozone, with the advantage that the measurements are also possible during the night. The first demonstration of tropospheric ozone column retrieval using the infrared domain was made using the IMG (Interferometric Monitor for Greenhouse gases) instrument (Turquety et al., 2002, Coheur et al., 2005). Later on, the TES (Tropospheric Emission Spectrometer) instrument aboard the EOS-Aura satellite has also provided measurements of tropospheric ozone (Worden et al., 2007) with first applications to air quality (Jones et al., 2008) and climate modelling (Worden et al., 2008). Finally recently, using measurements from the European IASI (Infrared Atmospheric Sounding Interferometer) instrument aboard the Metop-A satellite (launched in October 2006), tropospheric ozone during the heat wave over Europe in summer 2007 has been observed and compared with balloon sondes and predictions from a photochemical tropospheric model (Eremenko et al., 2008), demonstrating the great potential of IASI measurements for air quality applications. It

IASI measurements of tropospheric ozone over Chinese megacities

G. Dufour et al.

Title Page

Abstract

Introduction

Conclusions

References

Tables

Figures



Back

Close

Full Screen / Esc

Printer-friendly Version

Interactive Discussion

is worth noticing indeed that in contrast to TES, IASI has an excellent spatial coverage and is therefore well suited for measurements of tropospheric ozone with an air quality focus.

In this paper, we investigate the ability of the IASI instrument to monitor lower tropospheric ozone over the surroundings of three Chinese megacities (regions limited to 5° in latitude and longitude around each city): the northern part of the North China Plain (Beijing), the Yangtze River Delta (Shanghai), and the Pearl River Delta (Hong Kong) (Fig. 1). In particular we evaluate the possibilities of retrieving the seasonal variations of tropospheric ozone and also of probing its day-to-day variations. These regions have been selected because they enclose the largest Chinese megacities and large industrial regions (the Pearl River Delta is the world's major consumer goods manufacturing base) and because they lie in different latitudes from the tropics to the midlatitudes. The analyses are based on the first complete year of IASI operation: the year 2008. In the second section, the IASI instrument is described and the retrieval procedure is summarized. The third and fourth sections report on the seasonal variations of tropospheric ozone observed by IASI in the three regions and on its day-to-day variations, respectively.

2 The IASI observations

2.1 The IASI instrument

The IASI (Infrared Atmospheric Sounding Interferometer) (Clerbaux et al., 2007) instrument is a nadir-viewing spectrometer onboard the European MetOp-A satellite. This satellite, launched in October 2006, flies in a polar sun-synchronous orbit (about 800 km altitude) and crosses the equator at two fixed local solar times 9:30 a.m. (descending mode) and 9:30 p.m. (ascending mode). The IASI instrument is a Fourier-transform spectrometer with a 2-cm optical path difference covering the 645–2760 cm⁻¹ spectral range. The apodized spectral resolution is 0.5 cm⁻¹ (full-width at

IASI measurements of tropospheric ozone over Chinese megacities

G. Dufour et al.

Title Page

Abstract

Introduction

Conclusions

References

Tables

Figures

⏪

⏩

◀

▶

Back

Close

Full Screen / Esc

Printer-friendly Version

Interactive Discussion

IASI measurements of tropospheric ozone over Chinese megacities

G. Dufour et al.

Title Page

Abstract

Introduction

Conclusions

References

Tables

Figures

⏪

⏩

◀

▶

Back

Close

Full Screen / Esc

Printer-friendly Version

Interactive Discussion

half-maximum). The radiometric accuracy in noise-equivalent radiance temperature at 280 K is 0.28 K at 650 cm^{-1} and 0.47 K at 2400 cm^{-1} . IASI measures the thermal infrared radiation emitted by the Earth's surface and the atmosphere. The instrument scans the surface perpendicular to the satellite's flight track with 15 individual views on each side of the track (across-track). The maximum scan angle of 48.3° from the nadir corresponds to coverage of about 2200 km across-track for one swath.

The distance between two successive overpasses is 25° in longitude (i.e. 2800 km at the equator). Then, for latitudes higher than 45° , the footprints of two successive overpasses overlap. At the nadir point, the ground pixel size (total field-of-view) is $50 \times 50\text{ km}^2$. The total field-of-view is composed of 4 individual ground pixels with 12 km diameter each.

The primary objectives of the IASI instrument are to deliver meteorological products (surface temperature, temperature and humidity profiles, and cloud information). However the large spectral coverage, the high radiometric sensitivity and accuracy, and the rather high spectral resolution of the instrument allow deriving global distributions of several important trace gases (such as O_3 , CO , NH_3 , ...) at high spatial resolution (e.g. Eremanko et al., 2008; Turquety et al., 2009; Clarisse et al., 2009).

2.2 The retrieval method

The retrievals are performed using the radiative transfer model KOPRA (Karlsruhe Optimised and Precise Radiative transfer Algorithm) and its inversion module KOPRAFIT (Stiller et al., 2000), both adapted to the nadir-viewing geometry. A constrained least squares fit method with an analytical altitude-dependent regularization is used. The regularization method applied as well as the error calculations are detailed in Eremanko et al. (2008). To summarize, the regularization matrix is a combination of zero, first and second order Thikonov constraints (Tikhonov, 1963) with altitude-dependent coefficients. The coefficients are optimized both to maximize the degrees of freedom (DOF) of the retrieval and to minimize the total error on the retrieved profile. For the Beijing region the regularization matrix used in this study is the same as the one used

**IASI measurements
of tropospheric
ozone over Chinese
megacities**

G. Dufour et al.

Title Page

Abstract

Introduction

Conclusions

References

Tables

Figures

⏪

⏩

◀

▶

Back

Close

Full Screen / Esc

Printer-friendly Version

Interactive Discussion

in Eremenko et al. (2008), i.e. determined for summer midlatitude conditions. Note that the results of a validation study (Keim et al., 2009) show that, while the regularization matrix was built up for the summer period, it is valid as well also for the other seasons. Shanghai and Hong Kong lie in the tropics and the altitude-dependent regularization defined for the midlatitudes is not well adapted in this case, especially because the tropopause height is higher in the tropics. Accordingly a regularization matrix has then been set for the tropical conditions using the same procedure as for the midlatitudes (Eremenko et al., 2008). The a priori profiles used during the retrievals are compiled from the climatology of McPeters et al. (2007) and are typical for the midlatitudes (Beijing) and for the 20–40° N and the 10–30° N latitude bands for Shanghai, and Hong Kong, respectively. The same a priori profile has been used for all seasons.

The analysis of IASI data is performed in three steps. First, the effective surface temperature is retrieved from selected spectral windows between 800 and 950 cm⁻¹ assuming a blackbody with an emissivity equal to unity. In the second step, the atmospheric temperature profile is retrieved from CO₂ lines in the 15 μm spectral region and using the ECMWF profiles as a priori. In the third step, the ozone profiles are retrieved from seven spectral windows located in the 975–1100 cm⁻¹ region, that avoid strong water vapor lines. The spectroscopic parameters of the different species are from HITRAN 2004 (Rothman et al., 2005). Note that before starting the retrievals, the IASI spectra are filtered for cloud contamination. The cloud filter is based on tests on the retrieved surface temperature and on the shape of the baseline of the spectra (Eremenko et al., 2008). Only spectra for clear sky conditions are considered. A quality flag is also applied to the retrieved products to discard unphysical results (negative values, large oscillations).

The error budget, calculated for individual retrieved profile (see Eq. (3) in Eremenko et al., 2008) accounts for errors due to the measurement noise, the uncertainty in the temperature profile, the smoothing error and all the other systematic errors (e.g. uncertainty in spectroscopy). The corresponding total error in each retrieved concentration is about 30% on average from the surface up to 6 km and ranges between 35 and 45%

IASI measurements of tropospheric ozone over Chinese megacities

G. Dufour et al.

Title Page

Abstract

Introduction

Conclusions

References

Tables

Figures

⏪

⏩

◀

▶

Back

Close

Full Screen / Esc

Printer-friendly Version

Interactive Discussion

from 6 km up to the tropopause. The main contribution to the total error is the smoothing error. The total error in the columns is calculated from the error budget determined for the profile (see Eq. (4) in Eremenko et al., 2008). In fact the error on each retrieved concentration translates to a total error onto the 0–6 km columns that ranges from 10 to 20% – corresponding to less than 3 Dobson Units (DU) – for the 3 cities considered in the paper. A validation exercise performed over the first one-year-and-a-half of IASI operation for the northern midlatitudes shows that no significant bias (less than 5%) exists in the retrieved columns and that the errors derived from the error budget calculation are consistent with the standard deviation of the differences between sonde measurements and IASI observations (Keim et al., 2009). Examples of tropospheric averaging kernels are presented in Fig. 2 for each of the three megacities considered in the present study. Figure 2 suggests that the ozone from the lower and the upper troposphere can be separated from the IASI observations. The limit between these two distinguishable parts of the troposphere is about 6 km for Beijing and about 8–9 km for Shanghai and Hong Kong (Fig. 2). The averaging kernels of the lower tropospheric ozone have a maximum between 2 and 3 km for Beijing and a little higher (between 3 and 4 km) for Shanghai and Hong Kong. Nevertheless, there are not two really independent pieces of information in the troposphere. Indeed, the degrees of freedom range between 1.4 and 1.8 in the cases displayed in Fig. 2. Note that the retrieved ozone products are profiles but due to the lack of vertical sensitivity, we mainly present partial tropospheric columns in this paper.

3 Seasonal variation of tropospheric ozone over Beijing, Shanghai, and Hong Kong

Ozone in the troposphere presents an annual cycle that varies as a function of the location (Monks, 2000; Logan, 1999; Vingarzan, 2004). Monks (2000) reports in a detailed review that surface ozone exhibits a spring maximum in the northern Europe and at coastal sites whereas continental sites and high-altitude mountain sites show a

broad summer maximum. Zbinden et al. (2006) report on climatological measurements made within the MOZAIC framework (Marengo et al., 1998) and show that tropospheric ozone presents a broad summer maximum over different European and North American cities. This broad summer maximum is mainly attributed to photochemical production. In East Asia, the seasonal variations of surface and tropospheric ozone are not driven by the same processes especially during the summer monsoon. Several studies report on these seasonal variations at different locations of Eastern China and Japan (e.g. Chan et al., 1998; Naja and Akimoto, 2004; Kim et al., 2006; Li et al., 2007; Ding et al., 2008; He et al., 2008). They show a sharp maximum in late spring and a minimum during summer (July, August especially). The timing of the sharp maximum varies with longitude and altitude (Kim et al., 2006). Different processes can contribute to this maximum. A first hypothesis is the accumulation of ozone precursors during winter that are processed when radiation and temperature increase, coupled with an increase of photochemical production (Penkett and Brice, 1986; Penkett et al., 1993). Another process that can also contribute is the stratospheric-tropospheric exchange that can bring ozone-rich air from the stratosphere down to the free troposphere and the surface (Monks, 2000). In East China, biomass burning can also play a significant role in the increase of ozone and precursors in late spring and early summer (e.g. Liu et al., 1999; Pochanart et al., 2003). The key mechanism that contributes to the summer minimum is the intrusion of low-ozone marine air masses coming from the tropical Pacific (e.g. Lin et al., 2009). Actually, the flow direction becomes more southerly during the Asian summer monsoon bringing clean air masses from the Pacific (e.g. Ding et al., 2008; Liu et al; 2002). The influence of the summer monsoon is more pronounced in the South than in the North of China. A second maximum in fall is reported for measurements performed in Southern China, in the area of Hong Kong (Chan et al., 1998).

In this section, we present the monthly averaged tropospheric ozone (profiles and partial columns) for 2008 over the three regions considered: Beijing, Shanghai, and Hong Kong. Due to the decrease of the IASI coverage when going to the equator

**IASI measurements
of tropospheric
ozone over Chinese
megacities**

G. Dufour et al.

[Title Page](#)[Abstract](#)[Introduction](#)[Conclusions](#)[References](#)[Tables](#)[Figures](#)[⏪](#)[⏩](#)[◀](#)[▶](#)[Back](#)[Close](#)[Full Screen / Esc](#)[Printer-friendly Version](#)[Interactive Discussion](#)

(consecutive swaths do not overlap below 40° N) and due to the increase of cloud cover during the monsoon period, a satisfactory daily coverage for the considered area is difficult to reach especially in summer as shown by the percentages of cloud free and quality flagged columns considered for each city per month (Fig. 3). We then chose to calculate a global monthly average including all the data for each month without any pooling per day. We checked also that the monthly spatial coverage of the data was sufficiently homogeneous over each of the considered regions.

In Fig. 4, the monthly variations of the 0–6 km ozone column are compared to the climatological monthly variations for the corresponding latitude bands calculated from the McPeters et al. (2007) climatology. The climatological variabilities attached to each climatological monthly mean are also plotted in Fig. 4. Note that the climatological partial columns considered here are determined for latitude bands, including longitudes outside Asia. Then, the climatological columns do not especially reflect the Asian monsoon influence contrary to the IASI observations.

3.1 Beijing area

Previous studies report on the influence of the Asian summer monsoon up to Northern China, Korea and Japan (e.g. Ding et al., 2008; Naja and Akimoto, 2004; Kim et al., 2006). Ding et al. (2008) present a climatology of tropospheric ozone over Beijing based on aircraft data from the MOZAIC program. They show that the influence of the summer monsoon is more pronounced in the lowest layers of the troposphere with a sharp decrease in July for the layer between the surface and 600 m (note that IASI is not very sensitive to the ozone surface layer, Fig. 2). The maximum broadens for higher altitudes and the decrease is smoothed. The sharp maximum in May-June at the surface level leaves place to a broad summer maximum between 4 and 8 km (see Fig. 4 in Ding et al., 2008). The monthly mean 0–6 km partial columns of ozone observed by IASI in 2008 over Beijing (39.90° N, 116.39° E) are shown in the top panel of Fig. 4. The IASI observations show a maximum in May followed by a smooth de-

IASI measurements of tropospheric ozone over Chinese megacities

G. Dufour et al.

Title Page

Abstract

Introduction

Conclusions

References

Tables

Figures

⏪

⏩

◀

▶

Back

Close

Full Screen / Esc

Printer-friendly Version

Interactive Discussion

**IASI measurements
of tropospheric
ozone over Chinese
megacities**

G. Dufour et al.

Title Page

Abstract

Introduction

Conclusions

References

Tables

Figures

◀

▶

◀

▶

Back

Close

Full Screen / Esc

Printer-friendly Version

Interactive Discussion

crease to finally reach a minimum in early winter. This smooth decrease (Fig. 4) is consistent with the MOZAIC climatology with a smooth decrease starting in June (Ding et al., 2008). Similar seasonal cycles with an ozone maximum in early summer are visible at most of the tropospheric altitudes from the monthly mean profiles (Fig. 5a): the maximum is shifting from May to June between 5 and 7 km. The one-month delay in the ozone maximum is likely related to the time needed for the transport between the lowest layers of the troposphere and the free/upper troposphere as already noticed by Kim et al. (2006). This suggests, as already mentioned in Sect. 2, that typical behaviours of the lower troposphere and of the upper troposphere seem to be retrievable independently from the IASI observations, although the number of independent pieces of information are limited in the troposphere (smaller than 2 for the whole troposphere, Fig. 2). For a detailed view of the one-month delay, we plotted two individual levels representative of the lower and free troposphere (3 and 8 km respectively) in Fig. 6. Comparison with the climatology given for the 40–50° N latitude band at 3 km (Fig. 6) shows:

1. broader maximum for the climatology. The difference between the duration of the summer maximum of the climatology and of the IASI measurement over Beijing illustrates the impact of the Asian summer monsoon in the Beijing area. Indeed, the flow of clean air imported from the Pacific reduces the ozone level during summer in the lower troposphere.
2. The ozone concentration is up to 10 ppbv larger during the April to July period over Beijing than the climatological values for the 40–50° N latitude band that should represent background ozone in the latitude band. The largest value (about 70 ppbv) is in agreement with the climatological values derived from the MOZAIC measurements above Beijing (Ding et al., 2008). However, the significance of these enhancements of ozone over Beijing compared to climatological ozone cannot be firmly attributed to the sounding of highly polluted air masses on the one hand because of the errors that arise from the IASI retrievals (see Sect. 2.2) and

on the other hand because of the variability associated to each monthly climatological value.

Large tropospheric ozone columns are observed in February 2008 compared to January 2008 and March 2008 and to the climatology (Fig. 4). The monthly mean for the beginning of 2009 are added in Fig. 4 (stars) for comparison and do not exhibit a similar enhancement in February. A possible explanation for the enhanced 0-6 km columns observed in February 2008 is a descent of stratospheric air rich in ozone: large values in February are observed up to the stratosphere (Fig. 5a). Note also that the difference between the mean columns observed in March 2008 and March 2009 are certainly not related to different geophysical conditions between the two years but more certainly arises from a sampling issue of IASI. In March 2008, observations were made only during the first half of March whereas the 2009 observations were made during the whole month of March 2009.

Figure 7 shows the monthly mean 0–6 km columns of ozone, resolved in space, in the region of Beijing. The seasonal cycle is also well visible with a maximum in May but with additional information on the spatial distribution of ozone in the area. The largest ozone columns are observed over the northern part of the North China Plain and are located in the vicinity of the most populated parts of the region as expected. As mentioned previously, the explanation of these large ozone columns is a combination of several processes: photochemical production from local anthropogenic sources but also from biomass burning sources, activation of precursors accumulated during winter, and stratospheric-tropospheric exchange. Dedicated model studies will be necessary to identify the relative contribution of each process.

3.2 Shanghai area

The monthly mean 0–6 km columns of ozone over the Shanghai area (31.13° N, 121.27° E) are reported in the middle panel of Fig. 4 and compared to the corresponding climatologies for the 20–30° N and 30–40° N latitude bands. A seasonal cycle with a

IASI measurements of tropospheric ozone over Chinese megacities

G. Dufour et al.

Title Page

Abstract

Introduction

Conclusions

References

Tables

Figures

⏪

⏩

◀

▶

Back

Close

Full Screen / Esc

Printer-friendly Version

Interactive Discussion



**IASI measurements
of tropospheric
ozone over Chinese
megacities**

G. Dufour et al.

[Title Page](#)[Abstract](#)[Introduction](#)[Conclusions](#)[References](#)[Tables](#)[Figures](#)[⏪](#)[⏩](#)[◀](#)[▶](#)[Back](#)[Close](#)[Full Screen / Esc](#)[Printer-friendly Version](#)[Interactive Discussion](#)

affected by the Asian monsoon (shown by the 20–30° N latitude band, Fig. 8). The one-month shift of the maximum has already been discussed above. The ozone concentrations retrieved from IASI are nevertheless closer to those of the 30–40° latitude band, especially after the drop in July (Fig. 8 and 4). One explanation of this is that the Shanghai area is more influenced by air masses coming from northern latitudes with characteristics similar to the 30–40° N latitude band. Another possible explanation can also be that air masses observed by IASI over Shanghai during this period (August to October) are affected by local enhanced photochemical production due to pollution (and/or biomass burning). This second hypothesis suggests an anthropogenic origin of the second maximum observed over Shanghai in early fall, as reported for the Hong Kong area (Liu et al., 2002).

The monthly mean spatial distribution of the 0–6 km ozone columns measured with IASI is displayed in Fig. 9. The June maximum shown in Fig. 4 is also well visible in Fig. 9 with the maxima mainly located along the Yangtze River where the density of population is the largest one.

3.3 Hong Kong area

The monthly mean 0–6 km columns of ozone over the Hong Kong area (22.25° N, 114.17° E) are reported in the bottom panel of Fig. 4 and compared to the corresponding climatology of the 10–20° N and 20–30° N latitude bands. The seasonal cycle of ozone as shown by the IASI columns exhibits one maximum in May and a second significant maximum in September–October. The agreement with the climatological column values is rather good but with smaller IASI columns during winter (January to April). The ozone maximum observed with IASI (May) occurs at the same time as the one derived from the climatology for the 20–30° N latitude band. On the other hand it is shifted by one month as compared to the 10–20° N latitude band. However, it is to be noted that the climatology for the 10–20° N latitude band provided by McPeters et al. (2007) is based only on the Hilo station (19.7° N, 155° W) and might not be fully representative of all the longitudes. Concerning the second ozone maximum observed

IASI measurements of tropospheric ozone over Chinese megacities

G. Dufour et al.

Title Page

Abstract

Introduction

Conclusions

References

Tables

Figures

⏪

⏩

◀

▶

Back

Close

Full Screen / Esc

Printer-friendly Version

Interactive Discussion



IASI measurements of tropospheric ozone over Chinese megacities

G. Dufour et al.

Title Page

Abstract

Introduction

Conclusions

References

Tables

Figures

⏪

⏩

◀

▶

Back

Close

Full Screen / Esc

Printer-friendly Version

Interactive Discussion

with IASI in fall, several studies based on time series performed at a surface site or with ozone sonde measurements close to Hong Kong report also such a maximum in fall (Chan et al., 1998; Lam et al., 2001; Wang et al., 2009) mainly in the two lowest kilometres (Chan et al., 1998). This maximum is attributed to a photochemical production due to pollution (Liu et al., 2002). IASI retrieved columns and concentrations of ozone (Figs. 4 and 10) are significantly larger than those of the climatologies. This would be consistent with the anthropogenic origins of the observed maximum (Liu et al., 2002). The IASI observations suggest that the ozone maxima in late spring and fall persist up to about 10 km (Fig. 5c) and the seasonal cycle presents a broad summer maximum for upper altitudes (Fig. 10). Again, these results show the ability of discriminating between the lower and the upper tropospheric seasonal cycle of ozone with the IASI observations despite the small degrees of freedom of the IASI retrievals in the troposphere (Fig. 2). However, the persistence of the second ozone maximum up to 10 km in the Hong Kong case needs further investigations as this maximum is only reported for the lowest layers in literature. It might be partly due to the low vertical resolution of IASI.

The monthly mean spatial distribution of the 0–6 km ozone columns measured with IASI is displayed in Fig. 11. The late spring maximum is well visible with the largest ozone columns in the vicinity of the main cities of the area. The maximum in fall is especially visible in September and the largest ozone columns are also close to the main cities, suggesting a photochemical production. During winter the distribution of ozone columns is rather uniform in the Hong Kong region.

4 Day to day variation of tropospheric ozone over Beijing and Shanghai

In the previous section, we showed that, using IASI measurements, it is possible to derive seasonal variations of tropospheric ozone representative of the lower troposphere. In this section, we investigate the possibility of retrieving the day to day variation of tropospheric ozone over the three megacities considered. Concerning the Hong Kong

area, the temporal coverage of the satellite instrument at this latitude leads to gaps between consecutive swaths and then to gaps in the daily coverage of the Hong Kong region. This, combined with significant cloud cover especially during summer, does not allow following the day-to-day evolution of tropospheric ozone in this region. On the contrary the temporal coverage of the IASI satellite instrument improves with the latitude and becomes satisfactory for the regions of Shanghai and Beijing allowing one to follow the daily variations of tropospheric ozone over these two spatial regions.

The upper panels of Figs. 12 and 13 show the mean daily 0–6 km ozone columns over Beijing during February and April, respectively. The bottom parts of these figures show the spatial distribution of the columns for 4 selected days (red circles) during which events of large tropospheric ozone amounts are detected with IASI. The analysis of the mean daily profiles retrieved for the 4-days period (Fig. 14) shows large ozone values in the stratosphere and low ozone values in the troposphere on 7 February. This changes to large ozone values in both troposphere and stratosphere on 8 February and is followed by lower values in both the troposphere and the stratosphere on 9 and 10 February. This suggests that the large concentrations observed in the lower troposphere on 8 February are due to a descent of stratospheric air for this specific day. In April the situation is different, the stratospheric values are similar for the 4 days. Only the tropospheric part of the ozone profiles is enhanced on 16 and 17 April, suggesting that the large ozone tropospheric amounts are from various tropospheric origins: pollution with enhanced photochemical production, biomass burning, etc. The fact that a large number of cloudy pixels are detected during the last day of the period indicates that the meteorological situation has changed. The polluted air masses could have been mixed with clean air masses or/and washout by rain implying a reduction of ozone amounts as observed on 18 April. This would support the tropospheric origins of the ozone episode detected for this period.

For the Shanghai region (Fig. 15) we have identified one interesting case from 3 June to 6 June during which large ozone columns are observed with IASI, mainly along the Yangtse River (where the population density is the largest, see Fig. 1). The analysis

IASI measurements of tropospheric ozone over Chinese megacities

G. Dufour et al.

Title Page

Abstract

Introduction

Conclusions

References

Tables

Figures

⏪

⏩

◀

▶

Back

Close

Full Screen / Esc

Printer-friendly Version

Interactive Discussion

of the mean daily profiles retrieved for these 4 days (Fig. 14) shows: similar lower tropospheric ozone for the first two days, 3 and 4 June, whereas the lower tropospheric ozone amounts are smaller on 5 and 6 June, but with similar upper tropospheric – lower stratospheric (UTLS) ozone concentrations as on the 4 June. This supports a lower tropospheric origin (pollution with enhanced photochemical production, etc.) for the enhanced ozone concentrations on the 3 and 4 June. However, the UTLS ozone concentrations on 4 June are larger than on 3 June and this may also imply that some of the large ozone concentrations observed in the 0–6 km range have a higher-altitude origin.

5 Conclusions

In this paper we have studied one year of IASI observations of tropospheric ozone over three Chinese megacities and their surroundings ($5^{\circ} \times 5^{\circ}$ in latitude and longitude around each city). The monthly mean variations of lower tropospheric ozone measured with IASI (partial columns and profiles) show the influence of the summer Asian monsoon on the ozone concentrations with a sharp maximum in late spring and early summer (May–June) followed by a decrease during summer. The intensity of this decrease depends on the latitude: the drop is sharper for the tropical latitudes (Hong Kong and Shanghai) than for the midlatitudes (Beijing).

Moreover, the ozone values as observed by IASI, given either as partial columns or as concentrations for the given altitude, are larger than the ozone values derived from climatologies. Despite the fact that the error budgets associated with the retrievals show errors slightly larger than the difference observed with the climatology, it is worth noting that a validation study (Keim et al., 2009) does not reveal any significant systematic bias in the IASI retrievals (<5%). Thus, one can consider that these differences with the climatologies are significant in particular when considering monthly averages. Larger ozone values are especially observed in spring/summer (April to June) in Beijing and in early fall (September–October) corresponding to the second maximum detected

IASI measurements of tropospheric ozone over Chinese megacities

G. Dufour et al.

Title Page

Abstract

Introduction

Conclusions

References

Tables

Figures

⏪

⏩

◀

▶

Back

Close

Full Screen / Esc

Printer-friendly Version

Interactive Discussion

in Shanghai and Hong Kong. One hypothesis to explain the larger ozone amounts observed with IASI above the three largest Chinese cities is the enhanced photochemical production of ozone due to pollution events or biomass burning. These origins are already reported in the literature. The monthly mean spatial ozone distributions over the three megacities partly support the hypothesis of an anthropogenic origin of the large ozone amounts observed. Indeed, the large ozone amounts are rather well correlated with the largest populated areas.

Moreover, the spatial and temporal coverage of IASI observations allowed us to follow the daily variations (spatially resolved) of ozone over Beijing and Shanghai. Selected time periods with enhanced ozone detected with IASI have been analysed. We show that the large ozone amount observed in the lower troposphere during winter has likely a stratospheric origin. On the contrary, the large ozone amounts observed in the lower troposphere in spring and summer are more certainly related to an enhanced photochemical production of ozone linked to anthropogenic origins (pollution or biomass burning).

Finally, the results presented in this paper demonstrate the ability to discriminate, using the IASI measurements, between the different behaviours of the lower and the upper troposphere despite a limited number of degrees of freedom in the troposphere (around 1.5). This looks very promising for assessing air quality and transport of pollution.

IASI measurements of tropospheric ozone over Chinese megacities

G. Dufour et al.

Title Page

Abstract

Introduction

Conclusions

References

Tables

Figures



Back

Close

Full Screen / Esc

Printer-friendly Version

Interactive Discussion



Acknowledgements. We thank the Institut für Meteorologie und Klimaforschung (IMK), Karlsruhe, Germany, for a licence to use the KOPRA radiative transfer model, and especially M. Höpfner for his help to set up the code. We thank the ETHER database (CNRS, INSU, CNES) in France for providing access to IASI Level 1 data. This study was supported by the French Space Agency CNES (project “IASI-TOSCA”).



The publication of this article is financed by CNRS-INSU.

References

- Akimoto, H.: Global air quality and pollution, *Science*, 302, 1716–1719, 2003.
- Chan, L. Y., Liu, H. H. Y., Lam, K. S., Wang, T., Oltmans, S. J., and Harris, J. M.: Analysis of the seasonal behaviour of tropospheric ozone at Hong Kong, *Atmos. Environ.*, 32, 159–168, 1998.
- Center for International Earth Science Information Network (CIESIN), Columbia University, United Nations and Agriculture Programme (FAO), and Centro Internacional de Agricultura Tropical (CIAT): Gridded Population of the World: Future Estimates (GWPFE), Palisades, NY, Socioeconomic Data and Applications Center (SEDAC), Columbia University, available at: <http://sedac.ciesin.columbia.edu/gpw>, 2005 (last access: 17 July 2009).
- Clarisse, L., Clerbaux, C., Dentener, F., Hurtmans, D., and Coheur, P. F.: Global ammonia distribution derived from infrared satellite observations, *Nat. Geosci.*, 2, 479–483, 2009.
- Clerbaux, C., Hadji-Lazaro, J., Turquety, S., George, M., Coheur, P.-F., Hurtmans, D., Wespes, C., Herbin, H., Blumstein, D., Tournier, B., and Phulpin, T.: The IASI/MetOp I mission: First observations and highlights of its potential contribution to GMES, *Space Res. Today*, 168, 19–24, 2007.

ACPD

9, 23103–23140, 2009

IASI measurements of tropospheric ozone over Chinese megacities

G. Dufour et al.

Title Page

Abstract

Introduction

Conclusions

References

Tables

Figures

⏪

⏩

◀

▶

Back

Close

Full Screen / Esc

Printer-friendly Version

Interactive Discussion



**IASI measurements
of tropospheric
ozone over Chinese
megacities**

G. Dufour et al.

Title Page

Abstract

Introduction

Conclusions

References

Tables

Figures

◀

▶

◀

▶

Back

Close

Full Screen / Esc

Printer-friendly Version

Interactive Discussion

- Coheur, P.-F., Barret, B., Turquety, S., Hurtmans, D., Hadji-Lazaro, J., and Clerbaux, C.: Retrieval and characterization of ozone vertical profiles from a thermal infrared nadir sounder, *J. Geophys. Res.*, 110, D24303, doi:10.1029/2005JD005845, 2005.
- Ding, A. J., Wang, T., Thouret, V., Cammas, J.-P., and Nédélec, P.: Tropospheric ozone climatology over Beijing: analysis of aircraft data from the MOZAIC program, *Atmos. Chem. Phys.*, 8, 1–13, 2008, <http://www.atmos-chem-phys.net/8/1/2008/>.
- Eremenko, M., Dufour, G., Foret, G., Keim, C., Orphal, J., Beekmann, M., Bergametti, G., and Flaud, J.-M.: Tropospheric ozone distributions over Europe during the heat wave in July 2007 observed from infrared nadir spectra recorded by IASI, *Geophys. Res. Lett.*, 35, L18805, doi:10.1029/2008GL034803, 2008.
- Fishman, J., Ramanathan, V., Crutzen, P. J., and Liu, S. C.: Tropospheric ozone and climate, *Nature*, 282, 818–820, 1979.
- Fishman, J., Wozniak, A. E., and Creilson, J. K.: Global distribution of tropospheric ozone from satellite measurements using the empirically corrected tropospheric ozone residual technique: Identification of the regional aspects of air pollution, *Atmos. Chem. Phys.*, 3, 893–907, 2003, <http://www.atmos-chem-phys.net/3/893/2003/>.
- He, Y. J., Uno, I., Wang, Z. F., Pochanart, P., Li, J., and Akimoto, H.: Significant impact of the East Asia monsoon on ozone seasonal behavior in the boundary layer of Eastern China and the west Pacific region, *Atmos. Chem. Phys.*, 8, 7543–7555, 2008, <http://www.atmos-chem-phys.net/8/7543/2008/>.
- Jacob, D. J., Logan, J. A., and Murti, P. P.: Effect of rising Asian emissions on surface ozone in the United States, *Geophys. Res. Lett.*, 26, 2175–2178, 1999.
- Jones, D. B. A., Bowman, K. W., Horowitz, L. W., Thompson, A. M., Tarasick, D. W., and Witte, J. C.: Estimating the summertime tropospheric ozone distribution over North America through assimilation of observations from the Tropospheric Emission Spectrometer, *J. Geophys. Res.*, 113, D18307, doi:10.1029/2007JD009341, 2008.
- Keim, C., Eremenko, M., Orphal, J., Dufour, G., Flaud, J.-M., Höpfner, M., Boynard, A., Clerbaux, C., Payan, S., Coheur, P.-F., Hurtmans, D., Claude, H., Dier, H., Johnson, B., Kelder, H., Kivi, R., Koide, T., López Bartolomé, M., Lambkin, K., Moore, D., Schmidlin, F. J., and Stübi, R.: Tropospheric ozone from IASI: comparison of different inversion algorithms and validation with ozone sondes in the northern middle latitudes, *Atmos. Chem. Phys. Discuss.*, 9, 11441–11479, 2009, <http://www.atmos-chem-phys-discuss.net/9/11441/2009/>.

**IASI measurements
of tropospheric
ozone over Chinese
megacities**

G. Dufour et al.

Title Page

Abstract

Introduction

Conclusions

References

Tables

Figures

◀

▶

◀

▶

Back

Close

Full Screen / Esc

Printer-friendly Version

Interactive Discussion

- Kim, J. H., Lee, H. J., and Lee, S. H.: The characteristics of tropospheric ozone seasonality observed from ozone soundings at Pohang, Korea, *Environ. Monit. Assess.*, 118, 1–12, 2006.
- Lam, K. S., Wang, T. J., Chan, L. Y., Wang, T., and Harris, J.: Flow patterns influencing the seasonal behaviour of surface ozone and carbon monoxide at a coastal site near Hong Kong, *Atmos. Environ.*, 35, 3121–3135, 2001.
- Li, J., Wang, Z., Akimoto, H., Gao, C., Pochanart, P., and Wang, X.: Modeling study of ozone seasonal cycle in lower troposphere over east Asia, *J. Geophys. Res.*, 112, D22S25, doi:10.1029/2006JD008209, 2007.
- Lin, W., Xu, X., Zhang, X., and Tang, J.: Contributions of pollutants from North China Plain to surface ozone at the Shangdianzi GAW Station, *Atmos. Chem. Phys.*, 8, 5889–5898, 2008, <http://www.atmos-chem-phys.net/8/5889/2008/>.
- Lin, M., Holloway, T., Oki, T., Streets, D. G., and Richetr, A.: Mechanisms controlling surface ozone over East Asia: A multiscale study coupling regional and global chemical transport models, *Atmos. Chem. Phys.*, 9, 3277–3301, 2009, <http://www.atmos-chem-phys.net/9/3277/2009/>.
- Liu, H., Chang, W. L., Oltmans, S. J., Chan, L. Y., and Harris, J. M.: On springtime high ozone events in the lower troposphere from Southeast Asian biomass burning, *Atmos. Environ.*, 33, 2403–2410, 1999.
- Liu, H., Jacob, D. J., Chan, L. Y., Oltmans, S. J., Bey, I., Yantosca, R. M., Harris, J. M., Duncan, B. N., and Martin, R. V.: Sources of tropospheric ozone along the Asian Pacific Rim: an analysis of ozonesonde observations, *J. Geophys. Res.*, 107, 4573, doi:10.1029/2001JD002005, 2002.
- Liu, X., Chance, K. V., Sioris, C. E., Spurr, R. J. D., Kurosu, T. P., Martin, R. V., and Newchurch, M. J.: Ozone profile and tropospheric ozone retrievals from Global Ozone Monitoring Experiment: Algorithm description and validation, *J. Geophys. Res.*, 110, D20307, doi:10.1029/2005JD006240, 2005.
- Logan, J. A.: An analysis of ozonesonde data for the troposphere: Recommendations for testing 3-D modes and development of gridded climatology for tropospheric ozone, *J. Geophys. Res.*, 105(D2), 16115–16149, 1999.
- Marenco, A., Thouret, V., Nedelec, P., Smit, H., Helten, M., Kley, D., Karcher, F., Simon, P., Law, K., Pyle, J., Poschmann, G., Wrede, R. V., Hume, C., and Cook, T.: Measurement of ozone and water vapour by Airbus in-service aircraft: the MOZAIC airborne program, an overview, *J. Geophys. Res.*, 103(D19), 25631–25642, 1998.

**IASI measurements
of tropospheric
ozone over Chinese
megacities**

G. Dufour et al.

[Title Page](#)[Abstract](#)[Introduction](#)[Conclusions](#)[References](#)[Tables](#)[Figures](#)[⏪](#)[⏩](#)[◀](#)[▶](#)[Back](#)[Close](#)[Full Screen / Esc](#)[Printer-friendly Version](#)[Interactive Discussion](#)

- McPeters, R. D., Labow, G. J., and Logan, J. A.: Ozone climatological profiles for satellite retrieval algorithms, *J. Geophys. Res.*, 112, D05308, doi:10.1029/2005JD006823, 2007.
- Monks, P. S.: A review of the observations and origins of the spring ozone maximum, *Atmos. Environ.*, 34, 3545–3561, 2000.
- 5 Naja, M. and Akimoto, H.: Contribution of regional pollution and long-range transport to the Asia-Pacific region: Analysis of long-term ozonesonde data over Japan, *J. Geophys. Res.*, 109, D21306, doi:10.1029/2004JD004687, 2004.
- Oltmans, S. J., Lefohn, A. S., Harris, J. M., Galbally, I., Scheel, H. E., Bodeker, G., Brunke, E., Claude, H., Tarsick, D., Johnson, B. J., Simmonds, P., Shadwick, D., Anlauf, K., Hayden, K., Schmidlin, F., Fujimoto, T., Akagi, K., Meyer, C., Nichol, S., Davies, J., Redondas, A., and Cuevas, E.: Long-term changes in tropospheric ozone, *Atmos. Environ.*, 40, 3156–3173, 2006.
- 10 Penkett, S. A. and Brice, K. A.: The spring maximum in photooxidants in the Northern Hemisphere troposphere, *Nature*, 319, 655–658, 1986.
- 15 Penkett, S. A., Blake, N. J., Lightmann, P., Mardr, A. R. W., Ancoyl, P., and Butcher, G.: The seasonal variation of nonmethane hydrocarbons in the free troposphere over the North Atlantic Ocean: Possible evidence for extensive reaction of hydrocarbons with the nitrate radical, *J. Geophys. Res.*, 98, 2865–2885, 1993.
- Pochanart, P., Akimoto, H., Kaji, Y., and Sukasem, P.: Regional background ozone and carbon monoxide variations in remote Siberia/East Asia, *J. Geophys. Res.*, 108(D1), 4028, doi:10.1029/21001JD001412, 2003.
- 20 Richter, A., Burrows, J. P., Nub, H., Granier, C., and Niemeier, U.: Increase in tropospheric nitrogen dioxide over China observed from space, *Nature*, 437, 129–132, 2005.
- Rothman, L. S., Jacquemart, D., Barbe, A., Chris Benner, D., Birk, M., Brown, L. R., Carleer, M. R., Chackerian Jr., C., Chance, K., Coudert, L. H., Dana, V., Devi, V. M., Flaud, J.-M., Gamache, R. R., Goldman, A., Hartmann, J.-M., Jucks, K. W., Maki, A. G., Mandin, J.-Y., Massie, S. T., Orphal, J., Perrin, A., Rinsland, C. P., Smith, M. A. H., Tennyson, J., Tolchenov, R. N., Toth, R. A., Vander Auwera, J., Varanasi, P., and Wagner, G.: The HITRAN 2004 molecular spectroscopic database, *J. Quant. Spectrosc. Ra.*, 96, 139–204, 2005.
- 30 Seinfeld, J. H. and Pandis, S. N.: *Atmospheric Chemistry and Physics, from Air Pollution to Climate Change*, John Wiley and Sons Inc., Toronto, Canada, 1997.
- Stiller, G. P. (Ed.) with contributions from v. Clarmann, T., Dudhia, A., Echle, G., Funke, B., Glatthor, N., Hase, F., Höpfner, M., Kellmann, S., Kemnitzer, H., Kuntz, M., Linden, A., Lin-

der, M., Stiller, G. P., and Zorn, S.: The Karlsruhe Optimized and Precise Radiative Transfer Algorithm (KOPRA), Vol. FZKA 6487 of Wissenschaftliche Berichte, Forschungszentrum Karlsruhe, Germany, 2000.

Tikhonov, A.: On the Solution of Incorrectly Stated Problems and a Method of Regularisation, Dokl. Acad. Nauk SSSR, 151, 501–504, 1963.

Turquety, S., Hadji-Lazaro, J., and Clerbaux, C.: First satellite ozone distributions retrieved from nadir high-resolution infrared spectra, Geophys. Res. Lett., 29, 2198, doi:10.1029/2002GL016431, 2002.

Turquety, S., Hurtmans, D., Hadji-Lazaro, J., Coheur, P.-F., Clerbaux, C., Josset, D., and Tsamalis, C.: Tracking the emission and transport of pollution from wildfires using the IASI CO retrievals: analysis of the summer 2007 Greek fires, Atmos. Chem. Phys., 9, 4897–4913, 2009, <http://www.atmos-chem-phys.net/9/4897/2009/>.

Vingarzan, R.: A review of surface ozone background levels and trends, Atmos. Environ., 38, 3431–3442, 2004.

Wang, T., Wei, X. L., Ding, A. J., Poon, C. N., Lam, K. S., Li, Y. S., Chan, L. Y., and Anson, M.: Increasing surface ozone concentrations in the background atmosphere of Southern China, 1994-2007, Atmos. Chem. Phys., 9, 6217–6227, 2009, <http://www.atmos-chem-phys.net/9/6217/2009/>.

Worden, H. M., Logan, J. A., Worden, J. R., Beer, R., Bowman, K., Clough, S. A., Eldering, A., Fisher, B. M., Gunson, M. R., Herman, R. L., Kulawik, S. S., Lampel, M. C., Luo, M., Megretskaia, I. A., Osterman, G. B., and Shephard, M. W.: Comparisons of Tropospheric Emission Spectrometer (TES) ozone profiles to ozonesondes: Methods and initial results, J. Geophys. Res., 112, D03309, doi:10.1029/2006JD007258, 2007.

Worden, H. M., Bowman, K. W., Eldering, A., and Beer, R.: Satellite measurements of the clear-sky greenhouse effect from tropospheric ozone, Nat. Geosci., 1, 305–308, doi:10.1038/ngeo182, 2008.

Xu, J., Zhu, Y., and Li, J.: Seasonal cycles of surface ozone and NO_x in Shanghai, J. Appl. Meteorol., 36, 1424–1429, 1997.

Zbinden, R. M., Cammas, J.-P., Thouret, V., Nédélec, P., Karcher, F., and Simon, P.: Mid-latitude tropospheric ozone columns from the MOZAIC program: climatology and interannual variability, Atmos. Chem. Phys., 6, 1053–1073, 2006, <http://www.atmos-chem-phys.net/6/1053/2006/>.

IASI measurements of tropospheric ozone over Chinese megacities

G. Dufour et al.

[Title Page](#)[Abstract](#)[Introduction](#)[Conclusions](#)[References](#)[Tables](#)[Figures](#)[⏪](#)[⏩](#)[◀](#)[▶](#)[Back](#)[Close](#)[Full Screen / Esc](#)[Printer-friendly Version](#)[Interactive Discussion](#)

IASI measurements
of tropospheric
ozone over Chinese
megacities

G. Dufour et al.

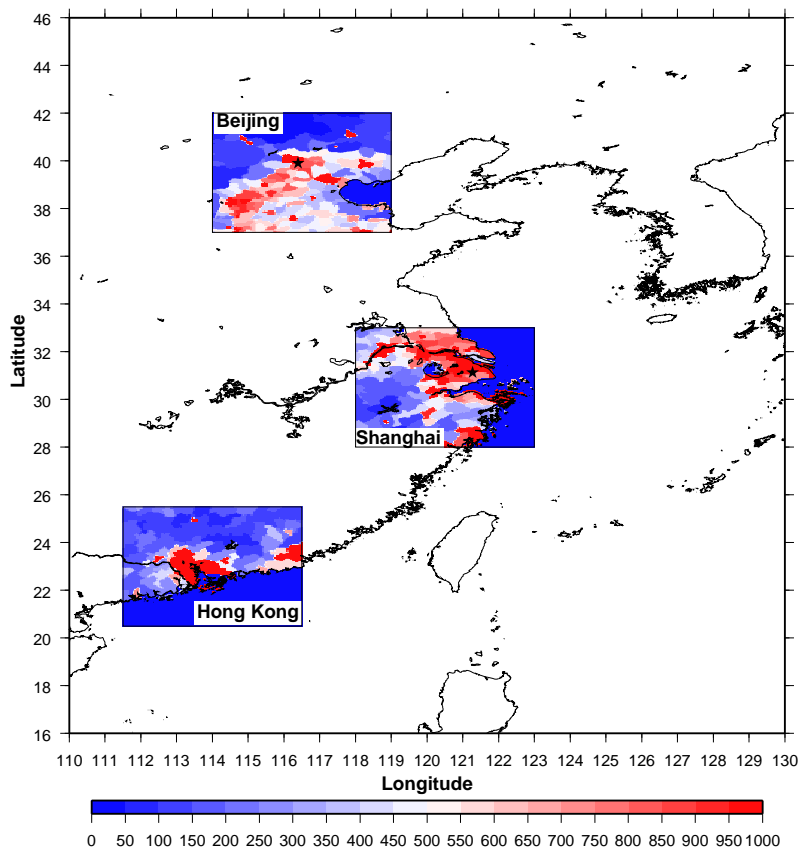


Fig. 1. Regions of $5^\circ \times 5^\circ$ in latitude and longitude around Beijing, Shanghai and Hong Kong considered for the present study with the population density indicated for each region. The population density, in persons/km², is given for 2005 (CIESIN, 2005).

[Title Page](#)[Abstract](#)[Introduction](#)[Conclusions](#)[References](#)[Tables](#)[Figures](#)[◀](#)[▶](#)[◀](#)[▶](#)[Back](#)[Close](#)[Full Screen / Esc](#)[Printer-friendly Version](#)[Interactive Discussion](#)

IASI measurements
of tropospheric
ozone over Chinese
megacities

G. Dufour et al.

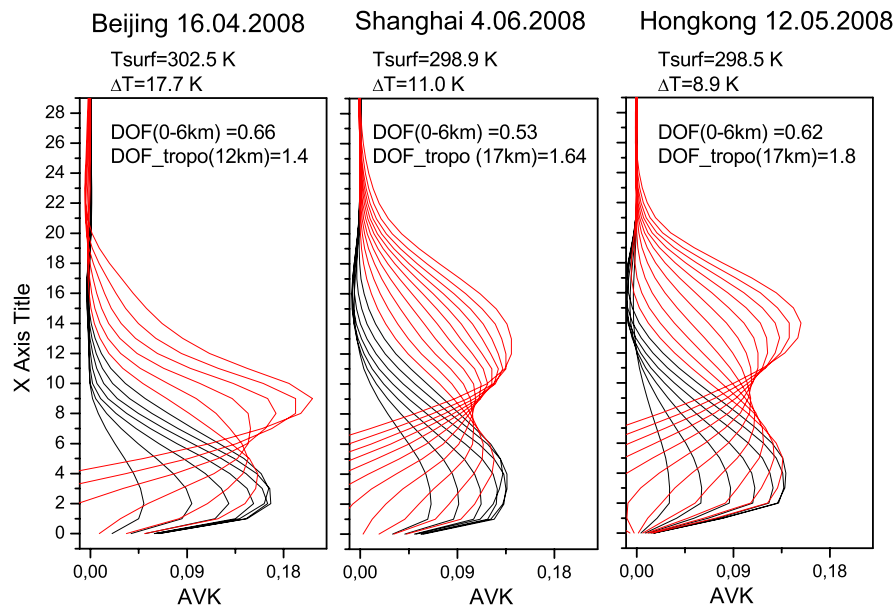


Fig. 2. Example of tropospheric averaging kernels derived from IASI observations above Beijing, Shanghai and Hong Kong. The retrieved surface temperature, the thermal contrast and the degrees of freedom up to 6 km and 12 km (Beijing) and 17 km (Shanghai and Hong Kong) are indicated for each case.

[Title Page](#)[Abstract](#)[Introduction](#)[Conclusions](#)[References](#)[Tables](#)[Figures](#)[⏪](#)[⏩](#)[◀](#)[▶](#)[Back](#)[Close](#)[Full Screen / Esc](#)[Printer-friendly Version](#)[Interactive Discussion](#)

**IASI measurements
of tropospheric
ozone over Chinese
megacities**

G. Dufour et al.

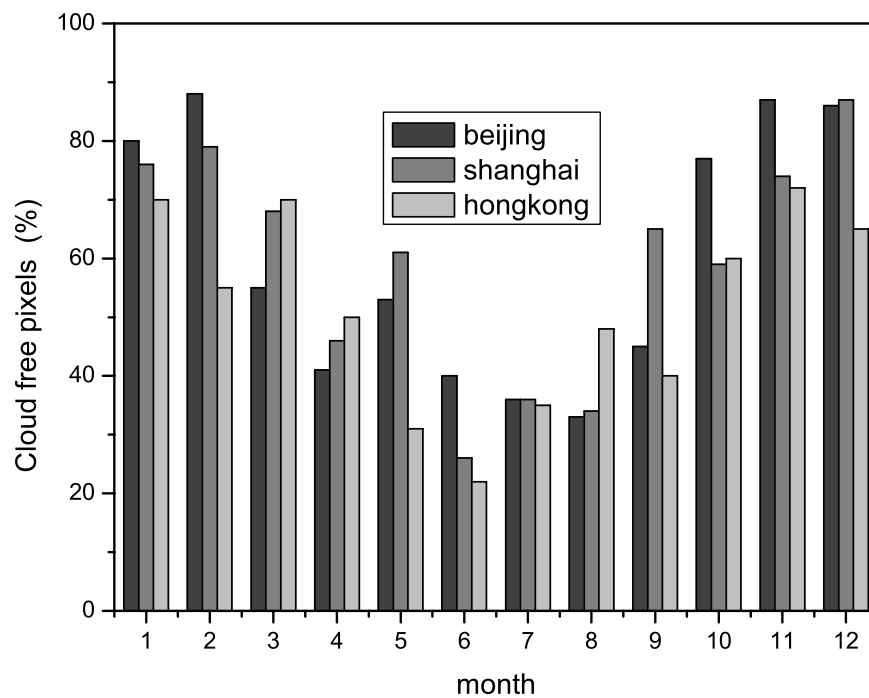


Fig. 3. Percentage of cloud free and ozone quality flagged IASI pixels per month for the 3 regions for the year 2008.

[Title Page](#)[Abstract](#)[Introduction](#)[Conclusions](#)[References](#)[Tables](#)[Figures](#)[◀](#)[▶](#)[◀](#)[▶](#)[Back](#)[Close](#)[Full Screen / Esc](#)[Printer-friendly Version](#)[Interactive Discussion](#)

IASI measurements
of tropospheric
ozone over Chinese
megacities

G. Dufour et al.

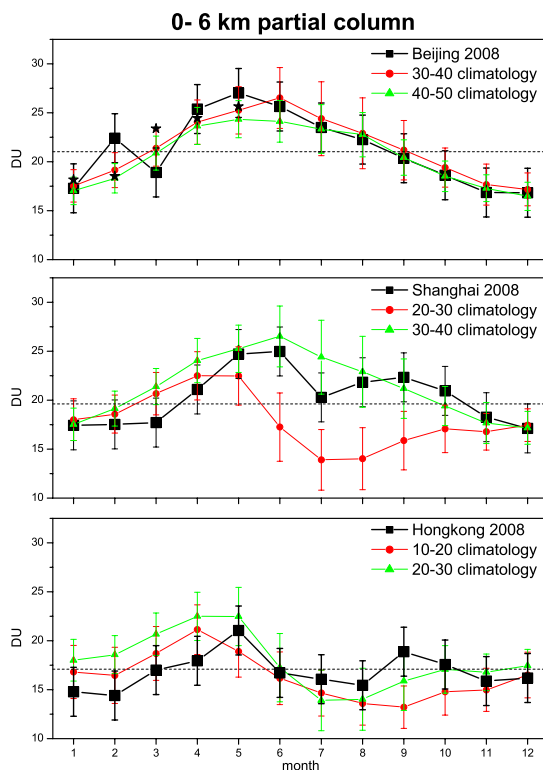


Fig. 4. Monthly variations of the mean 0–6 km ozone columns measured with IASI in 2008 over Beijing (top), Shanghai (middle), and Hong Kong (bottom), in Dobson Unit (DU). The mean columns are compared to the climatological column values (McPeters et al., 2007) for the corresponding upper and lower latitudes bands (green and red). The climatological variability is plotted as error bars for the climatological columns. The black stars in the top panel correspond to the monthly mean columns observed in 2009 over Beijing.

[Title Page](#)[Abstract](#)[Introduction](#)[Conclusions](#)[References](#)[Tables](#)[Figures](#)[◀](#)[▶](#)[◀](#)[▶](#)[Back](#)[Close](#)[Full Screen / Esc](#)[Printer-friendly Version](#)[Interactive Discussion](#)

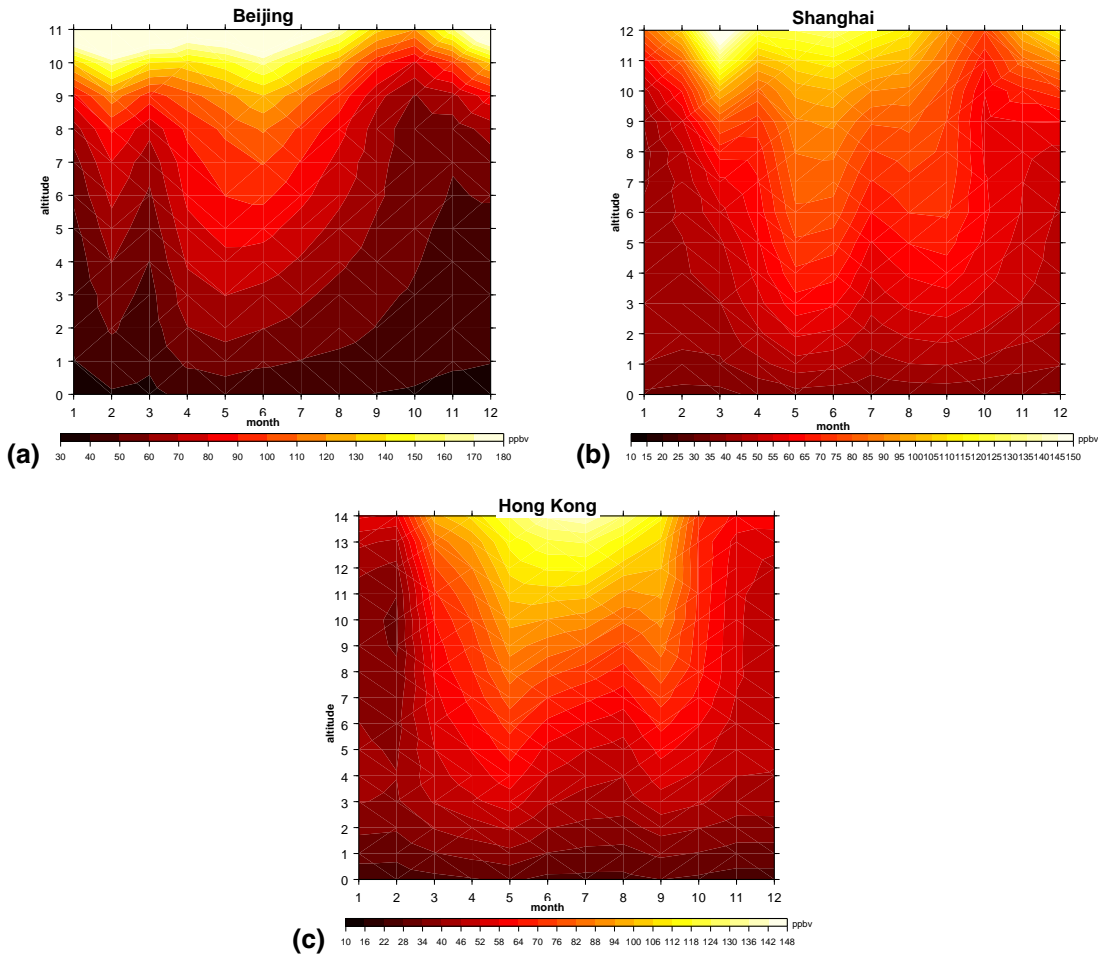


Fig. 5. Monthly mean ozone profiles retrieved from IASI in 2008 over Beijing **(a)**, Shanghai **(b)**, and Hong Kong **(c)** as a time function.

**IASI measurements
of tropospheric
ozone over Chinese
megacities**

G. Dufour et al.

Title Page

Abstract

Introduction

Conclusions

References

Tables

Figures

◀

▶

◀

▶

Back

Close

Full Screen / Esc

Printer-friendly Version

Interactive Discussion

IASI measurements
of tropospheric
ozone over Chinese
megacities

G. Dufour et al.

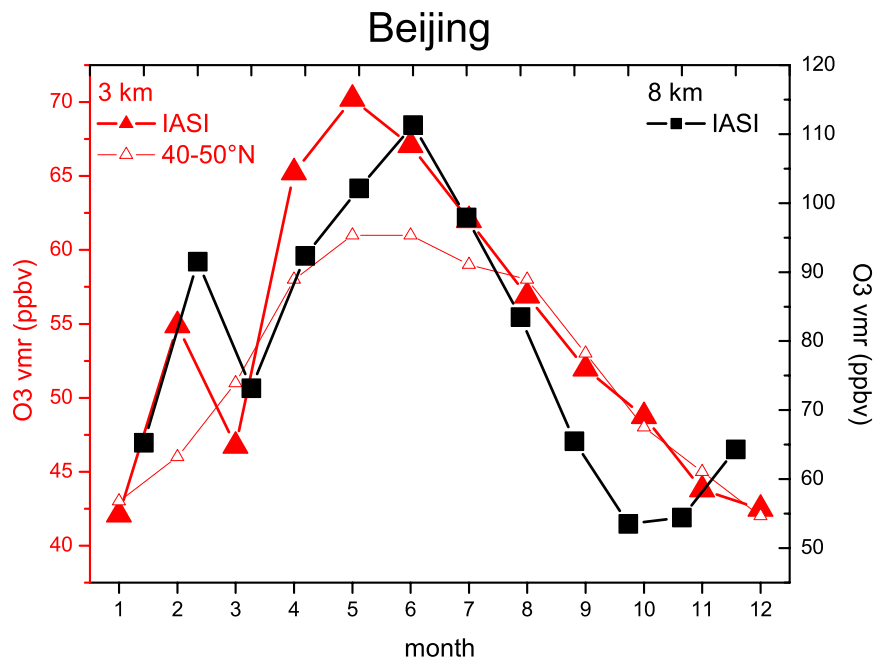


Fig. 6. Monthly mean variations of ozone volume mixing ratio (vmr) retrieved at 3 (red) and 8 (black) km from IASI observations over Beijing in 2008. The monthly mean ozone vmr at 3 km are compared to the monthly climatological values of the 40–50° N latitude band for the same level (McPeters et al., 2007).

[Title Page](#)[Abstract](#)[Introduction](#)[Conclusions](#)[References](#)[Tables](#)[Figures](#)[◀](#)[▶](#)[◀](#)[▶](#)[Back](#)[Close](#)[Full Screen / Esc](#)[Printer-friendly Version](#)[Interactive Discussion](#)

IASI measurements
of tropospheric
ozone over Chinese
megacities

G. Dufour et al.

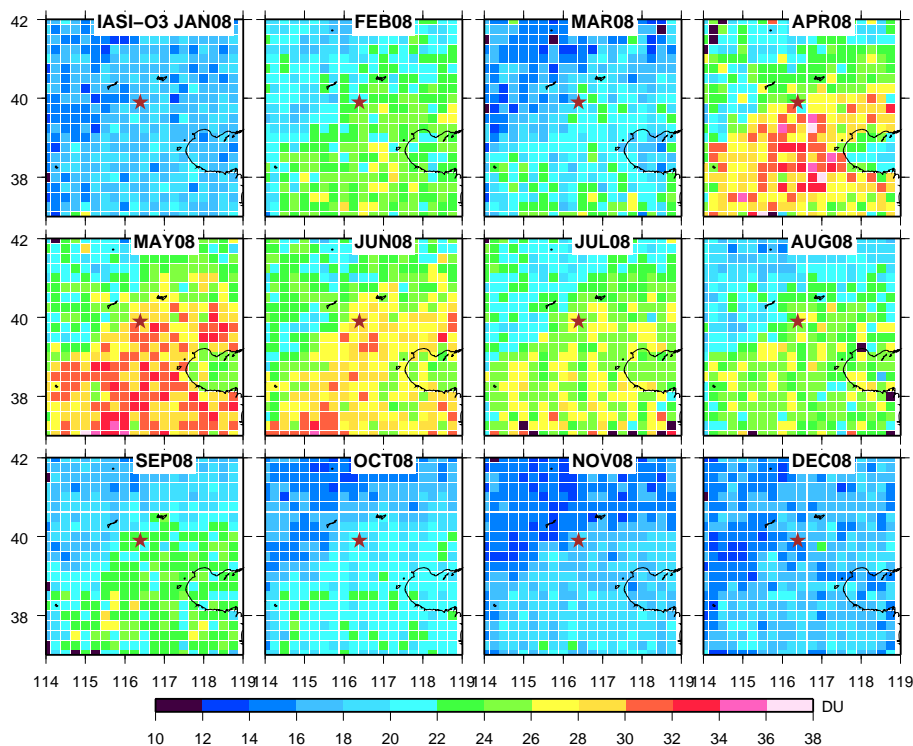


Fig. 7. Monthly mean 0–6 km ozone columns from IASI spatially averaged on a $0.25^\circ \times 0.25^\circ$ latitude-longitude grid for 2008 in the Beijing region (given in Dobson Unit, DU). Beijing location is indicated by a brown star. Black squares are displayed when no data is available in a grid cell.

[Title Page](#)[Abstract](#)[Introduction](#)[Conclusions](#)[References](#)[Tables](#)[Figures](#)[◀](#)[▶](#)[◀](#)[▶](#)[Back](#)[Close](#)[Full Screen / Esc](#)[Printer-friendly Version](#)[Interactive Discussion](#)

IASI measurements
of tropospheric
ozone over Chinese
megacities

G. Dufour et al.

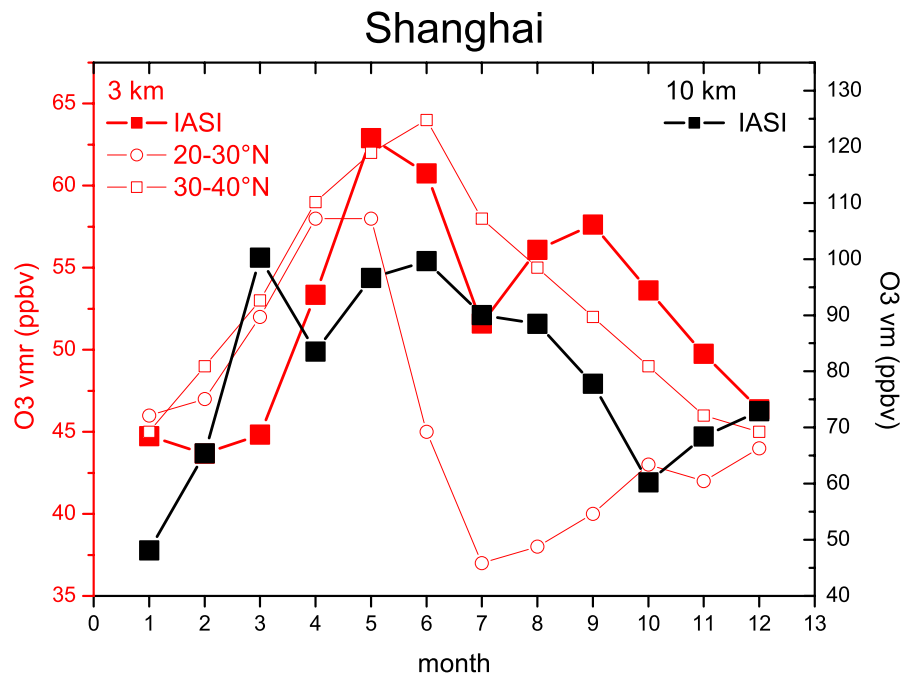


Fig. 8. Monthly mean variations of ozone vmr retrieved at 3 (red) and 10 km (black) from IASI observations over Shanghai in 2008. The monthly mean ozone vmrs at 3 km are compared to the monthly climatological values of the 20–30° N and 30–40° N latitude band for the same level (McPeters et al., 2007).

[Title Page](#)[Abstract](#)[Introduction](#)[Conclusions](#)[References](#)[Tables](#)[Figures](#)[⏪](#)[⏩](#)[◀](#)[▶](#)[Back](#)[Close](#)[Full Screen / Esc](#)[Printer-friendly Version](#)[Interactive Discussion](#)

IASI measurements
of tropospheric
ozone over Chinese
megacities

G. Dufour et al.

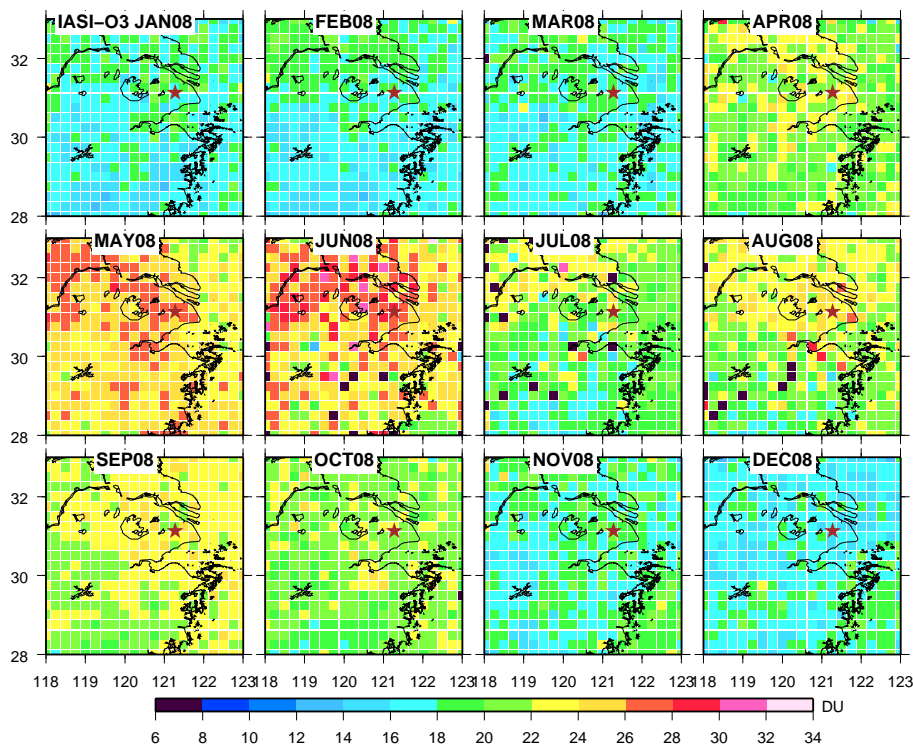


Fig. 9. Same as Fig. 7 for Shanghai.

[Title Page](#)[Abstract](#)[Introduction](#)[Conclusions](#)[References](#)[Tables](#)[Figures](#)[◀](#)[▶](#)[◀](#)[▶](#)[Back](#)[Close](#)[Full Screen / Esc](#)[Printer-friendly Version](#)[Interactive Discussion](#)

IASI measurements
of tropospheric
ozone over Chinese
megacities

G. Dufour et al.

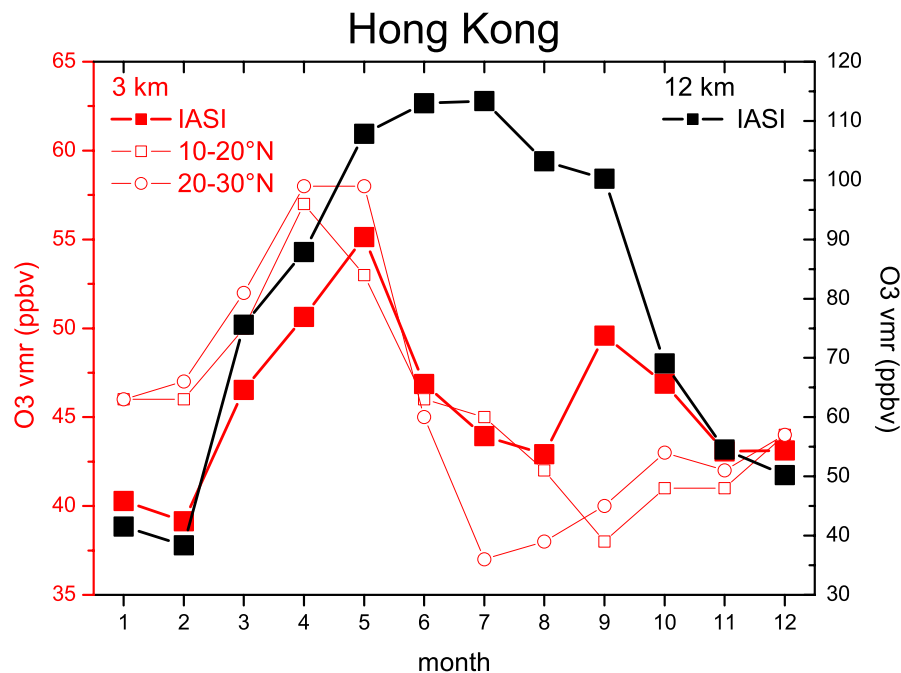


Fig. 10. Monthly mean variations of ozone vmr retrieved at 3 (red) and 12 km (black) from IASI observations over Hong Kong in 2008. The monthly mean ozone vmrs at 3 km are compared to the monthly climatological values of the 10–20° N and 20–30° N latitude band for the same level (McPeters et al., 2007).

[Title Page](#)[Abstract](#)[Introduction](#)[Conclusions](#)[References](#)[Tables](#)[Figures](#)[⏪](#)[⏩](#)[◀](#)[▶](#)[Back](#)[Close](#)[Full Screen / Esc](#)[Printer-friendly Version](#)[Interactive Discussion](#)

IASI measurements
of tropospheric
ozone over Chinese
megacities

G. Dufour et al.

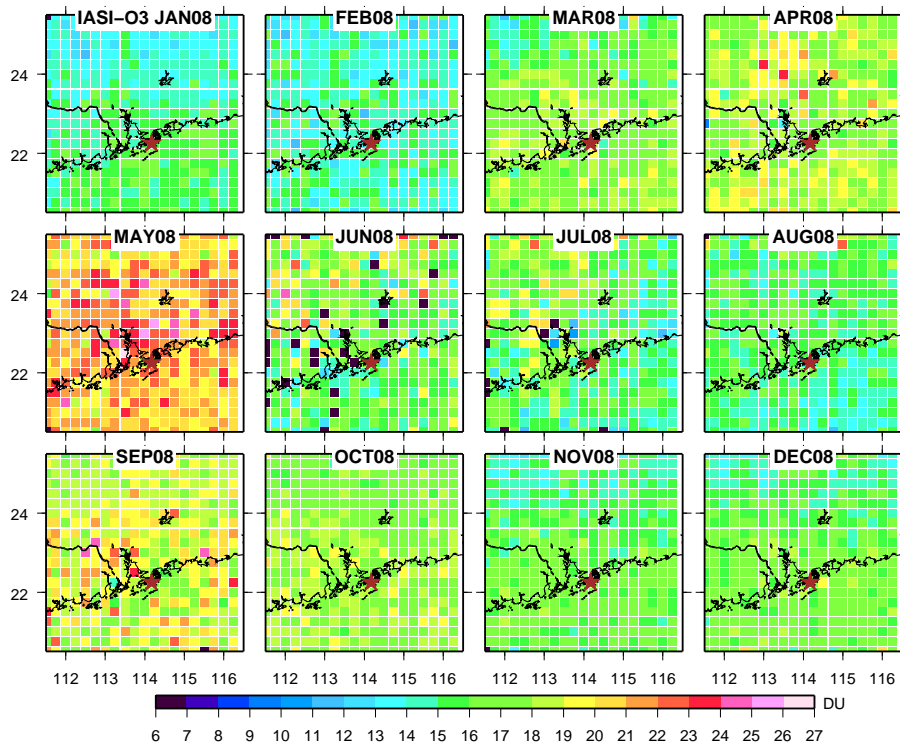


Fig. 11. Same as Fig. 7 for Hong Kong.

[Title Page](#)[Abstract](#)[Introduction](#)[Conclusions](#)[References](#)[Tables](#)[Figures](#)[⏪](#)[⏩](#)[◀](#)[▶](#)[Back](#)[Close](#)[Full Screen / Esc](#)[Printer-friendly Version](#)[Interactive Discussion](#)

IASI measurements
of tropospheric
ozone over Chinese
megacities

G. Dufour et al.

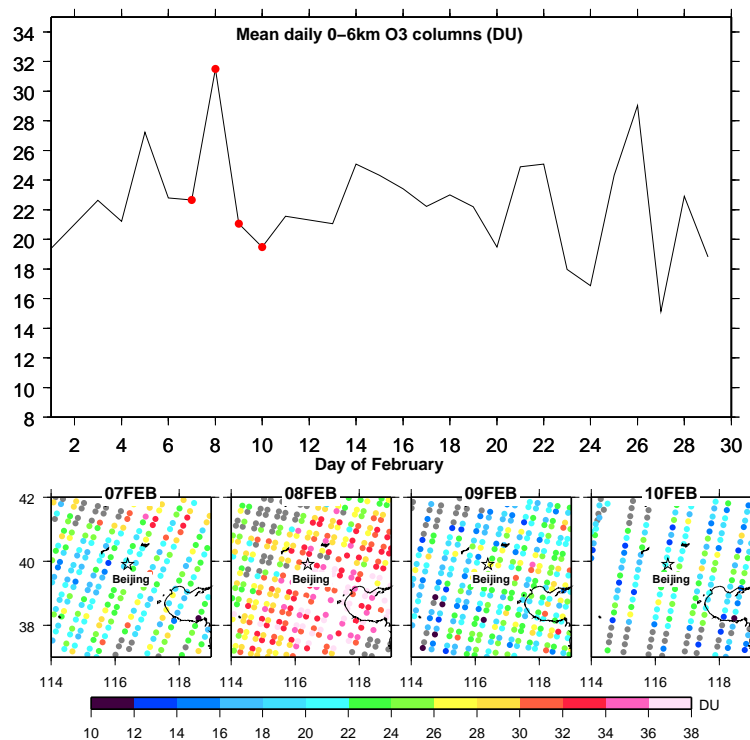


Fig. 12. Mean daily 0–6 km ozone columns (morning pass) retrieved from IASI over the Beijing region in DU (top). The corresponding spatial distribution of the partial columns for 4 selected days from 7 February to 10 February, marked with red dots in the upper panel, is plotted in the bottom. Each circle corresponds to one IASI pixel. Grey circles represent cloudy pixels.

[Title Page](#)[Abstract](#)[Introduction](#)[Conclusions](#)[References](#)[Tables](#)[Figures](#)[◀](#)[▶](#)[◀](#)[▶](#)[Back](#)[Close](#)[Full Screen / Esc](#)[Printer-friendly Version](#)[Interactive Discussion](#)

IASI measurements
of tropospheric
ozone over Chinese
megacities

G. Dufour et al.

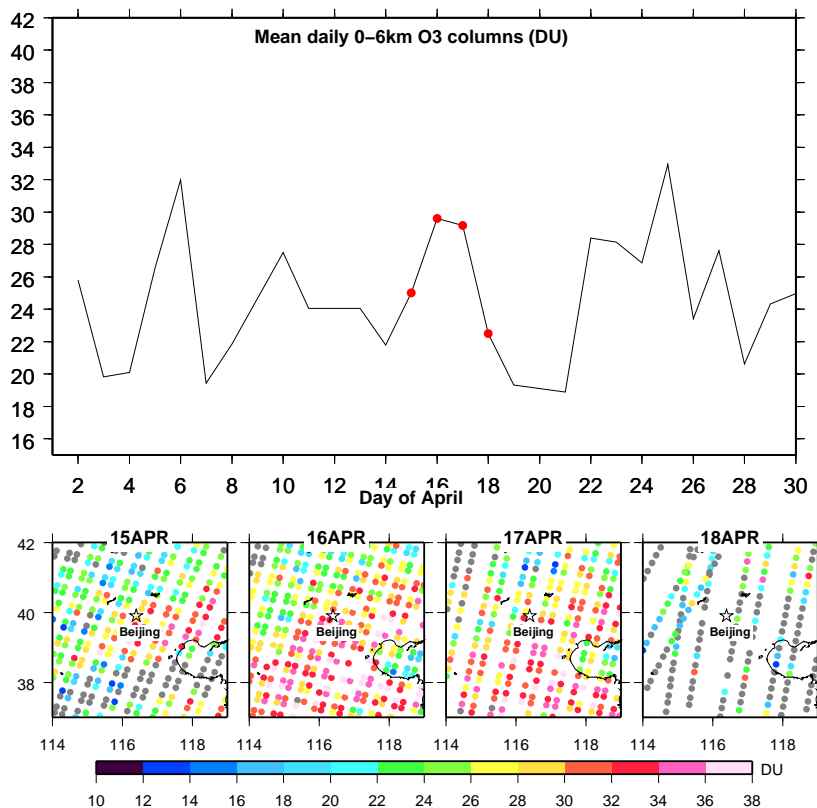


Fig. 13. Same as Fig. 12 for the period from 15 April to 18 April.

[Title Page](#)[Abstract](#)[Introduction](#)[Conclusions](#)[References](#)[Tables](#)[Figures](#)[◀](#)[▶](#)[◀](#)[▶](#)[Back](#)[Close](#)[Full Screen / Esc](#)[Printer-friendly Version](#)[Interactive Discussion](#)

IASI measurements
of tropospheric
ozone over Chinese
megacities

G. Dufour et al.

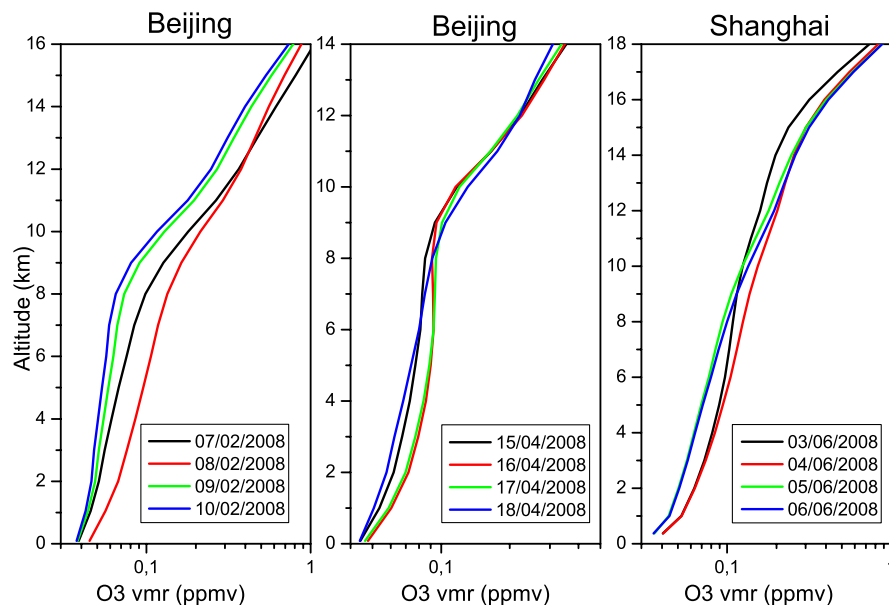


Fig. 14. Mean daily ozone profiles retrieved from IASI for the two selected periods with enhanced ozone events over Beijing and for one selected period over Shanghai.

[Title Page](#)[Abstract](#)[Introduction](#)[Conclusions](#)[References](#)[Tables](#)[Figures](#)[⏪](#)[⏩](#)[◀](#)[▶](#)[Back](#)[Close](#)[Full Screen / Esc](#)[Printer-friendly Version](#)[Interactive Discussion](#)

IASI measurements
of tropospheric
ozone over Chinese
megacities

G. Dufour et al.

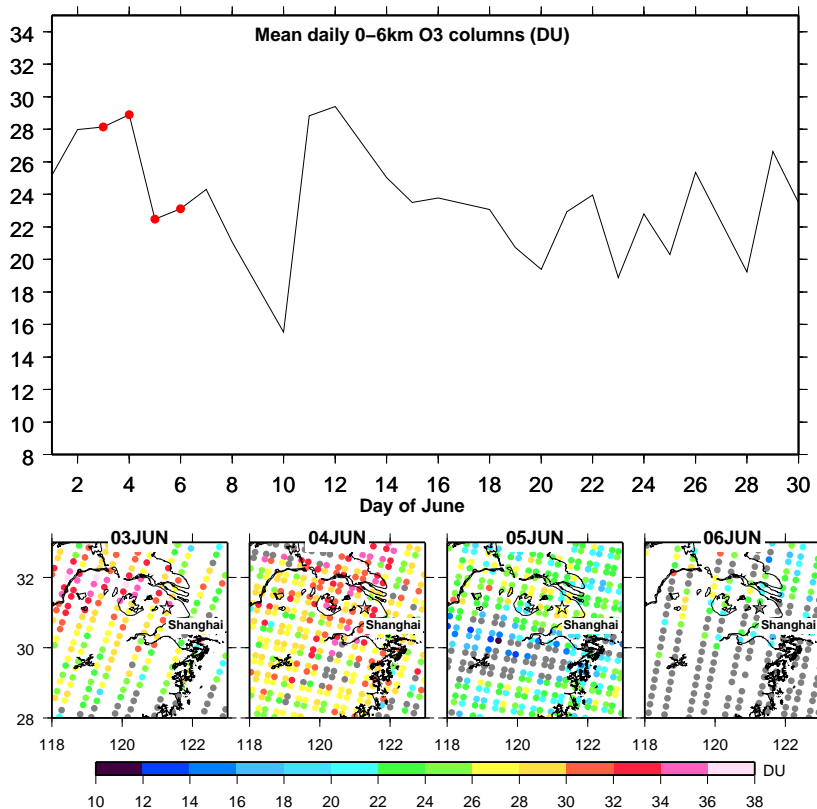


Fig. 15. Same as Fig. 12 for the Shanghai region and for the period from 3 June to 6 June.

[Title Page](#)[Abstract](#)[Introduction](#)[Conclusions](#)[References](#)[Tables](#)[Figures](#)[⏪](#)[⏩](#)[◀](#)[▶](#)[Back](#)[Close](#)[Full Screen / Esc](#)[Printer-friendly Version](#)[Interactive Discussion](#)